AD-A113 685   NAVAL RESEARCH LAB   WASHINGTON DC   F/G 18/3
                FISSION BETA PARTICLES EMITTED INTO THE GEOMAGNETOSPHERE.(U)
                APR 82   W L BENDEL
UNCLASSIFIED   NRL-MR-4712   NL

END
DATE
FILMED
5-82
DTIC

REPORT DOCUMENTATION PAGE	READ INSTRUCTIONS BEFORE COMPLETING FORM

1. REPORT NUMBER	2. GOVT ACCESSION NO.	3. RECIPIENT'S CATALOG NUMBER
NRL Memorandum Report 4712	AD-A113 685	

4. TITLE (and Subtitle)	5. TYPE OF REPORT & PERIOD COVERED
FISSION BETA PARTICLES EMITTED INTO THE GEOMAGNETOSPHERE	Interim report on a continuing NRL problem
	6. PERFORMING ORG. REPORT NUMBER

7. AUTHOR(s)	8. CONTRACT OR GRANT NUMBER(s)
W. L. Bendel	

9. PERFORMING ORGANIZATION NAME AND ADDRESS	10. PROGRAM ELEMENT, PROJECT, TASK AREA & WORK UNIT NUMBERS
Naval Research Laboratory Washington, DC 20375	61153N; RR0120141; 66-0439-0-2

11. CONTROLLING OFFICE NAME AND ADDRESS	12. REPORT DATE
	April 15, 1982
	13. NUMBER OF PAGES
	19

14. MONITORING AGENCY NAME & ADDRESS(if different from Controlling Office)	15. SECURITY CLASS. (of this report)
	UNCLASSIFIED
	15a. DECLASSIFICATION/DOWNGRADING SCHEDULE

16. DISTRIBUTION STATEMENT (of this Report)

Approved for public release; distribution unlimited.

17. DISTRIBUTION STATEMENT (of the abstract entered in Block 20, if different from Report)

18. SUPPLEMENTARY NOTES

19. KEY WORDS (Continue on reverse side if necessary and identify by block number)

Satellite shielding	Fission beta spectra
Electron shielding	Dose vs depth

20. ABSTRACT (Continue on reverse side if necessary and identify by block number)

The spectrum of electrons emitted into the earth's magnetic field by an exoatmospheric nuclear burst is considerably more energetic than the spectrum of all delayed electrons from fission, a spectrum often used. A better electron spectrum for general use is presented. Some items are calculated, including a depth-dose curve, for the two spectra compared.

DD FORM 1473 EDITION OF 1 NOV 65 IS OBSOLETE
1 JAN 73
S/N 0102-014-6601

CONTENTS

FISSION BETA PARTICLES
EMITTED INTO THE GEOMAGNETOSPHERE

Introduction

Electrons from exoatmospheric nuclear fission detonations are a major radiation threat to earth satellites. Past experience, notably following the Starfish test device detonated at 400 km above Johnston Island in 1962, shows that such electrons can destroy spacecraft in earth orbit. The dose within the spacecraft is often calculated from an assumed fission electron spectrum. The central purposes of this article are to show that a commonly-used threat electron spectrum is inappropriate, to present a better electron spectrum for general use when the specific threat weapon or spectrum is not known, and to present some results using these spectra.

There are a number of links in the chain of events from the nuclear burst to the radiation damage in spacecraft. In the instant following initiation of a fission or fusion explosion, many electrons are emitted. For the most part, these are absorbed in the device. The high energy electrons emitted later are primarily those from beta decay of fission fragments. While some electrons are also produced by internal conversion of the gamma rays following beta decay and by other processes, these are of lower energy. For these reasons, the spectrum of electrons from a nuclear device (with appreciable fission content) is generally taken to be a "fission beta spectrum". This is the distribution of electrons from all fission fragments, including daughter radioactivities.

Following an exoatmospheric nuclear explosion, radioactive fission fragments are present as isolated atoms or ions, and in droplets of material, charged or uncharged. As long as these specks of matter are outside of the atmosphere but within the magnetosphere, the beta radiation is emitted into a vacuum in the presence of a magnetic field. The electrons of interest in regard to radiation effects on orbiting spacecraft are, therefore, primarily the fission-fragment beta particles emitted relatively soon after the detonation. Many of these electrons, or beta rays, will be trapped in the magnetic field, spiraling back and forth along a flux line.

For some results presented in "The Trapped Radiation Handbook" (ref. 1), such as the depth-dose curve for normally-incident fission electrons (Fig. 8-31), "the shape of the energy spectrum of the injected trapped electrons is assumed to be constant in space and time and is represented by the fission electron energy spectrum of Carter ..." (p. 8-58). This spectrum is from thermal neutrons on ^{235}U. As the results of Carter et al. (ref. 2) do not extend below 1 MeV or above 7 MeV, extensions of the spectrum must be adopted before the dose per electron can be calculated.

More importantly, Carter et al. use beta decays for infinite time after fission rather than for the first few minutes.

We are not interested in all beta particles emitted by the detonation of a nuclear weapon. We are interested only in the spectrum of those emitted at the proper time after the chain reaction. In the first millisecond or so, any free electron will encounter atoms of the surrounding material and probably be absorbed. After a few minutes, any electron freed from an atom of the weapon will probably be in the earth's atmosphere, on the earth's surface, or embarked on a tour of the solar system. Only those electrons freed in the intermediate time range are candidates for trapping in the earth's magnetic field and, therefore, a threat to orbiting spacecraft. We shall adopt the period of 0 to 100 seconds after fission as the time period of relevant electron emission. (A time of 100 seconds yields a free-fall distance of 49 km. In an exoatmospheric nuclear explosion, much greater dispersion occurs in this period of time.)

In this report, we deal with the electron spectrum emitted into the geomagnetosphere. We do not evaluate the probability of an electron of given energy entering a trapped trajectory. With additional assumptions of long particle lifetime in the magnetosphere, long orbit mission, and equivalent electron trajectories, the emitted electron spectrum can be considered to be the same as the bombarding electron spectrum. This assumption is made in Ref. 1, using the spectrum of Ref. 2, as implied in the quotation above.

The Energy Spectrum

The fission-fragment beta spectrum as a function of time may be obtained from a report by LaBauve et al. (ref. 3). Their Appendix C lists the beta and gamma ray powers, each for eleven energy ranges from 0.1 to 7.5 MeV; five types of neutron-induced fission are tabulated. The power in each range is given as the sum of about 16 fitted terms. Each term is of the form $\alpha e^{-\lambda t}$, the contribution of a single effective radioactive lifetime. A term is readily integrated to the form for energy release in a given time period. The number of particles (the quantity desired here) is not given directly. Both α and λ are given to six significant figures. This does not imply that degree of precision in the data leading to the fit. Similarly, the working values shown here carry more digits than the conditions justify. The final table carries fewer significant digits.

The beta energy release is distinctly unequal for the five cases -- thermal neutrons on ^{233}U, ^{235}U, and ^{239}Pu, plus fast neutrons on ^{232}Th and ^{238}U. The two fission fragments produced by neutrons on the isotope $^{A}_{Z}Xx$ are typically a total of about

$$n_1 + n_2 = 0.42 (A + 1.5) - Z$$

beta steps from the stability line and have an excess energy roughly proportional to the square of this quantity. The number of beta decays will

2

be somewhat less than this as a stable isotope is often produced before reaching the theoretical stability line. The data on energy per fission and on betas per fission are consistent with this line of reasoning, with about

$$N = n_1 + n_2 - 1.9$$

beta decays.

The beta particle spectrum is, of course, different for different nuclear weapons. Clearly, no one spectrum will fit all cases. In the absence of specific threat information, we shall take a reference source from the data of LaBauve. We adopt the spectrum obtained from equal numbers of fissions in ^{235}U, ^{238}U, and ^{239}Pu. Note that the effect of incident neutron energy is ignored.

Table 1 shows, for these three isotopes, the integrated beta energy as a function of time. In general, the fragments produced by fission of ^{238}U are furthest from the line of beta stability. The first beta decay is therefore a fast, high-energy transition. This is seen, in Table 1, as an excess energy release in ^{238}U in the first minute, followed by about the same release as with ^{235}U or ^{239}Pu at later times.

Table 1. Kinetic energy of the beta particles following neutron fission, in keV/fission, from fission to given times after fission. Only particles in the range 0.1 to 7.5 MeV are included.

Time	Thermal on ^{235}U	Fast on ^{238}U	Thermal on ^{239}Pu
0.1 sec	84	167	49
0.3 sec	227	448	133
1 sec	565	1101	340
3 sec	1073	2006	674
10 sec	1884	3203	1240
30 sec	2703	4298	1851
50 sec	3069	4765	2154
100 sec	3555	5359	2584
300 sec	4152	6051	3141
1000 sec	4700	6640	3671
1 hour	5198	7146	4141
4 hours	5555	7479	4439
1 day	5900	7773	4698
4 days	6019	7888	4813
14 days	6086	7953	4877
364 days	6237	8093	5012
∞	6345	8186	5098

Part of the results calculated from the data of LaBauve et al. are given in Table 2, showing energy in each of their eleven ranges of particle kinetic energy, T. The results for each isotope are shown, somewhat rounded, for the time period of 0 to 100 seconds after fission. The average over isotopes is also given for this time period and for infinite time (forever). These averages will be utilized below to obtain particle number distributions.

Table 2. Distribution of kinetic energy of the beta particles following neutron-induced fission, in keV/fission, according to LaBauve. The values in parentheses, however, are calculated from Table 3.

To 100 seconds after fission

Energy (MeV)	Thermal on ^{235}U	Fast on ^{238}U	Thermal on ^{239}Pu	Average "100 sec"	Average "Forever"
0.1 - 0.4	42.4	57.4	35.0	44.9	292.5
0.4 - 0.9	224.7	313.4	177.5	238.5	822.5
0.9 - 1.35	370.4	526.5	287.0	394.6	892.7
1.35- 1.8	485.6	700.2	368.8	518.2	949.9
1.8 - 2.2	471.9	701.6	357.8	510.4	815.0
2.2 - 2.6	465.3	705.2	349.6	506.7	738.7
2.6 - 3.0	406.6	623.0	301.2	443.6	613.9
3.0 - 4.0	654.3	1017.8	455.3	709.1	910.5
4.0 - 5.0	269.7	433.1	161.6	288.2	323.0
5.0 - 6.0	120.9	203.8	66.7	130.5	135.7
6.0 - 7.5	43.44	77.57	23.35	48.12	48.58
Subtotal, 0.1 - 7.5	3555.2	5359.5	2583.7	3832.8	6543.0
Part > 3.0	30.6%	32.3%	27.4%	30.7%	21.7%
0.0 - 0.1				(2.48)	(25.0)
7.5 - 9.0				(2.95)	(2.96)
Total				(3838.2)	(6571.0)

Any number of reference spectra could be generated by varying the time limits and the type of fission. Using the fraction of energy in particles with T > 3.0 MeV as a criterion, Table 2 shows that the variation between spectra of fissioning isotopes is appreciable but considerably less than that between the 100-second value and the integral to infinity. From Table 1, it is seen that little error is introduced into the beta emission spectrum by setting the lower time limit to zero. Whether the weapon is dispersed into 10^{-5} or 10^{-1} second, the beta emission before dispersal is a small fraction of the whole. The upper limit is more important, but not as important as appears at first glance. If the choice of 100 seconds is off by a factor of 2, the total energy emitted will be changed by 12%, but the spectral shape will remain nearly the same.

4

The Number Spectrum

Let us define the quantities

T = beta particle energy (MeV),
N = number of beta decays per fission,
y = beta particles per MeV per beta decay,
and $Y = yN$ = beta particles per MeV per fission.

The number of particles in an energy range is therefore

$$I = \int Y \, dT \quad \text{betas/fission.} \tag{1}$$

The values of LaBauve et al. are the energy integrals

$$E = \int Y \, T \, dT \quad \text{MeV/fission} \tag{2}$$

$$\text{or} \quad E = \int 1000 \, Y \, T \, dT \quad \text{keV/fission.} \tag{2a}$$

Equation (2a) was employed to obtain values of Y from the input data of Table 2. Two sets of values of the form

$$1000 \, Y = (9 - T) \, e^p, \tag{3}$$

$$\text{with} \quad p = a_0 + bT + cT^2, \tag{4}$$

were calculated. See Appendix A. The spectra, $1000 \, Y$ vs. T, and the difference spectrum are shown on Fig. 1.

The next step is to calculate N from Eq. (1). One may normalize to beta decays rather than fissions by letting

$$a = a_0 - \ln N. \tag{5}$$

One now has

$$1000 \, y = (9 - T) \, e^q, \tag{3a}$$

$$\text{where} \quad q = a + bT + cT^2. \tag{4a}$$

The values of N as well as a, b, and c are listed in Table 3. They also provide values below 0.1 and above 7.5 MeV, completing the spectrum in Table 2. These parameters will be used below in integrals of the form

$$Z_k = \int 1000y \, T^k \, dT \tag{6}$$

with $k = 0$, 1, and 2.

5

Table 3. Parameters of electron spectra, used in Eqs. (3a) and (4a).

Energy (MeV)	a	b	c
Average "100-second" spectrum, $N = 2.1998$			
0.0 - 0.9	3.15126	1.20059	-0.5760
0.9 - 1.8	3.25839	0.84773	-0.3162
1.8 - 3.0	2.96243	0.97705	-0.2967
3.0 - 4.0	4.08434	0.17618	-0.1544
4.0 - 5.0	12.97099	-4.12788	0.3662
5.0 - 9.0	0.78733	0.95685	-0.1634
Average "forever" spectrum, $N = 5.7516$			
0.0 - 0.9	4.65034	-1.12004	0.1468
0.9 - 1.8	4.01274	-0.17724	-0.1136
1.8 - 3.0	3.52121	0.20203	-0.1726
3.0 - 4.0	3.75389	0.10107	-0.1648
4.0 - 5.0	13.16325	-4.48807	0.3944
5.0 - 9.0	0.38056	0.80647	-0.1532

The average "100-second" spectrum has $N = 2.1998$ beta particles per fission. The integrals of Eq. (6), as normalized to beta decays in Table 3, may be evaluated over the complete range of $T = 0$ to 9 MeV. The results are $Z_0 = 1000$ (by normalization), $Z_1 = 1744.83$, and $Z_2 = 4399.37$. That is, $\overline{T}$ is 1.745 MeV and T_{rms} is 2.097 MeV.

The average "forever" spectrum has $N = 5.7516$ beta particles per fission. As normalized, the integrals are 1000, 1142.46, and 2409.97, with $T_{rms} = 1.552$ MeV. While the beta energy per fission increases from 3.8 MeV in the first 100 seconds to a total of 6.5 MeV, the beta energy per particle decreases from 1.7 MeV to 1.1 MeV.

Quantized Spectra

In order to facilitate applied calculations, such as radiation doses, it is useful to replace a continuous electron spectrum with an equivalent discrete (or delta-function) spectrum. This was done by evaluating the integrals over each energy bin of all three forms of Eq. (6), then setting the integrals equal to the corresponding sums of discrete components at three energies. See Appendix B. The results with 0.5 MeV spacings are tabulated in Table 4.

Table 4. Discrete fission beta spectrum components D, versus energy T. Each case is averaged over three isotopes and normalized to 1000 particles.

Energy T (Mev)	Average "100 sec"	Average "forever"
0.0	44	157
0.5	176	333
1.0	171	151
1.5	170	122
2.0	147	88
2.5	112	63
3.0	76	39
3.5	46	22
4.0	25.0	11.5
4.5	14.0	6.0
5.0	8.5	3.4
5.5	5.3	2.0
6.0	3.0	1.3
6.5	1.3	0.5
7.0	0.6	0.1
7.5	0.2	0.2
8.0	0.1	0.0
Total, $\sum D$	1000 particles	1000
$\sum DT$	1744.60 MeV	1142.25
$\sum DT^2$	4399.30 $(MeV)^2$	2410.08

Depth vs. Dose Curve

A spacecraft, moving in an earth orbit and bombarded by electrons spiraling in the earth's magnetic field, is subjected to an isotropic distribution of electrons. (The electron penetration will not be as great as shown in Fig. 8-31 of Ref. 1, which involves normal incidence.) We pursue the dose, using the geometry of a semi-infinite plane -- a slab. An exposure of, for example, 2×10^8 omnidirectional electrons/cm^2 means that 2×10^8 electrons strike a sphere of cross-section $\pi r^2 = 1$ cm^2. If isotropic, this is 10^8 half-space isotropic electrons/cm^2, but the flux through unit surface is only half that number, 5×10^7 electrons/cm^2.

The energy deposition of isotropic monoenergetic electrons in aluminum has been determined by Watts and Burrell,[4] based on Monte Carlo calculations. When smoothed as described in Appendix C, one obtains Tables 5 and 6. The energy deposition is given at depths which are a fraction, F, of the average electron pathlength, P. Following Ref. 4, we use the

7

pathlengths of Berger and Seltzer.[5] For any other low-Z material, Tables 5 and 6 may be used with the relevant pathlength by correcting for the energy deposition relative to Al. One may use Ref. 5 or the more recent article by Pages et al.[6]

The discrete spectra of Table 4 may be combined with the depth-dose tables, producing the fission beta dose curves of Fig. 2. At sufficient depth, the average energy deposition per electron by the "forever" spectrum is only 0.4 that of the "100 sec" spectrum. (In spite of the 0.5-MeV steps in the spectra employed, the results are quite accurate between 0.2 and 4 g/cm^2.) By comparison with Fig. 11 of Ref. 4, it is seen that each spectrum reaches the level of bremsstrahlung dosage at a depth of 3.0 g/cm^2.

Summary

The spectrum of electrons emitted into the earth's magnetic field by an exoatmospheric nuclear burst is quite different from the spectrum of all delayed electrons from fission. Using the spectra calculated here as representing these cases, it is seen that the early electrons have about 53 percent more energy per electron and can therefore produce 53 percent more dose on a spacecraft. Only about one electron in 2.6 is emitted in the early time period, but almost all high energy electrons are emitted at early times. Thus the dose per electron at certain shielding depths could change by a factor of 2.6. This is confirmed in Fig. 2. The dose per electron at the surface is rather insensitive to the spectral shape.

The replacement of the "forever" spectrum by the "100 second" spectrum is a significant step in obtaining a realistic injected electron threat for components within earth satellites in the absence of detailed calculations employing specific weapon output spectra and radiation belt capture and loss mechanisms. The short-time spectrum should also be used when specific weapon information is known. The replacement of a continuous electron spectrum by groups of electrons at discrete energies simplifies dose calculations.

Acknowledgment

8

Table 5. Energy deposition, keV/gram per half-space isotropic electron, at a depth of F pathlengths in an aluminum slab as a function of energy.

F	.5 MeV	1 MeV	2 MeV	3 MeV	4 MeV	5 MeV	6 MeV	10 MeV
.01	2129	1828	1716	1678	1675	1657	1659	1645
.03	2144	1818	1703	1668	1657	1648	1655	1643
.05	2147	1800	1666	1638	1620	1616	1620	1602
.07	2105	1769	1609	1589	1582	1573	1566	1545
.09	2057	1722	1566	1540	1531	1523	1519	1498
.11	2004	1676	1535	1505	1482	1464	1479	1455
.13	1969	1642	1495	1467	1444	1429	1441	1425
.15	1927	1626	1466	1429	1409	1419	1411	1395
.17	1901	1609	1442	1389	1371	1402	1388	1362
.19	1866	1566	1398	1343	1337	1346	1344	1330
.21	1820	1500	1351	1301	1298	1280	1280	1290
.23	1764	1434	1301	1267	1256	1242	1238	1244
.25	1730	1382	1253	1224	1220	1222	1220	1205
.27	1665	1341	1211	1188	1183	1187	1188	1175
.29	1596	1293	1167	1144	1140	1141	1130	1148
.31	1538	1229	1122	1105	1102	1108	1079	1112
.33	1474	1161	1079	1072	1066	1077	1060	1077
.35	1408	1113	1025	1040	1031	1045	1046	1036
.37	1366	1080	985	997	993	1024	1013	985
.39	1310	1036	954	948	945	984	962	935
.41	1208	979	909	890	876	911	908	903
.43	1089	906	849	833	820	853	856	874
.45	1002	830	791	788	777	810	807	839
.47	944	770	736	742	738	753	754	792
.49	889	725	683	689	696	705	704	753
.51	806	656	624	635	649	663	663	717
.53	708	584	558	593	593	608	624	671
.55	627	525	498	536	539	552	582	622
.57	545	469	448	470	488	505	542	579
.59	456	393	391	415	441	465	501	538
.61	384	320	333	364	393	420	442	501
.63	318	272	290	314	348	361	384	467
.65	250	235	254	275	307	304	343	424
.67	205	192	211	233	268	262	309	375
.69	170	155	168	194	223	228	267	331
.71	134	126	133	164	181	195	229	295
.73	103	96.5	107	133	150	165	192	260
.75	78.2	73.9	87.1	102	124	138	159	219
.77	55.2	53.6	70.4	77.5	95.7	111	131	185
.79	39.9	37.1	51.8	58.8	73.1	85.7	107	156
.81				42.8	57.2	65.8	79.8	128
.83					43.2	48.3	56.7	101
.85							41.1	78.0
.87								58.8
.89								45.3

Table 6. Electron energy deposition, in keV/gram per half-space isotropic electron, at depths in aluminum nearly equal to the pathlength, P. Values are obtained from Eq. (C2).

F	.5 MeV	1 MeV	2 MeV	3 MeV	4 MeV	5 MeV	6 MeV	10 MeV
.81	23.5	25.1	32.3					
.83	14.4	16.2	21.8	28.9				
.85	8.1	9.8	14.0	19.4	29.4	34.9		
.87	4.1	5.4	8.5	12.3	20.1	24.5	30.9	
.89	1.7	2.7	4.7	7.3	13.2	16.5	21.4	
.91	0.6	1.1	2.3	4.0	8.1	10.6	14.3	31.8
.93	0.1	0.3	0.9	1.9	4.6	6.4	9.0	22.2
.95	0	0.1	0.3	0.7	2.4	3.5	5.3	14.9
.97		0	0	0.2	1.0	1.7	2.8	9.4
.99				0	0.3	0.7	1.3	5.6
1.01					0.1	0.2	0.5	3.1
1.03					0	0	0.1	1.5
1.05							0	0.6
1.07								0.2
1.09								0
D	0.962	0.979	0.999	1.015	1.045	1.058	1.072	1.115
k	17190	12660	10990	10610	8970	8500	8330	8140

Average Pathlength, gram/cm^2 Al

P	0.2243	0.5493	1.212	1.885	2.476	3.076	3.658	5.841

References

1.   J. B. Cladis, G. T. Davidson, and L. L. Newkirk, Eds., The Trapped
      Radiation Handbook, DNA 2524H, Defense Nuclear Agency, Washington, DC
      (Revised, 1977).

2.   R. E. Carter, F. Reines, J. J. Wagner, and M. E. Wyman, Phys. Rev.
      113, 280 (1959).

3.   R. J. LaBauve, T. R. England, D. C. George, and M. G. Stamatelatos,
      LA-7483-MS Informal Report, Los Alamos Scientific Lab. (Sep. 1978).

4.   J. W. Watts, Jr., and M. O. Burrell, "Electron and Bremsstrahlung
      Penetration and Dose Calculation," NASA TN D-6385 (1971).

5.   M. J. Berger and S. M. Seltzer, "Tables of Energy Losses and Ranges of
      Electrons and Positrons," NASA SP-3012 (1964). This work is also part
      of NAS-NRC Publication 1133 (1965). It covers 41 materials.

6.   L. Pages, E. Bertel, H. Joffre, and L. Sklavenitis, Atomic Data 4, 1
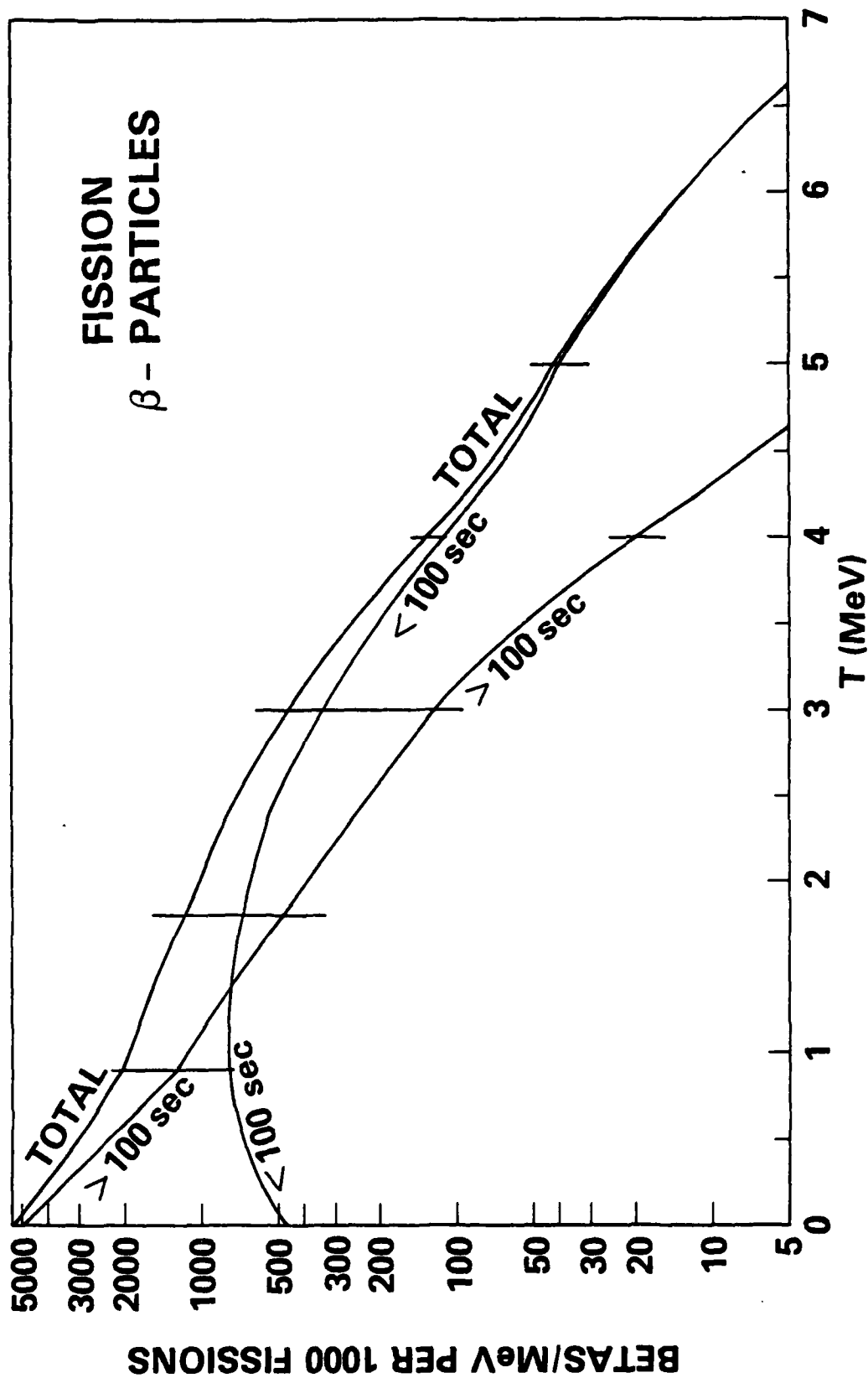   (1972). This article covers 115 materials.

Fig. 1 Spectrum of beta particles from equal numbers of fissions in ^{235}U, ^{238}U, and ^{239}Pu. The vertical lines mark the boundaries for the parameter sets of Table 3. Almost all high energy electrons are emitted within 100 seconds after fission; most of those under 1 MeV are emitted later.
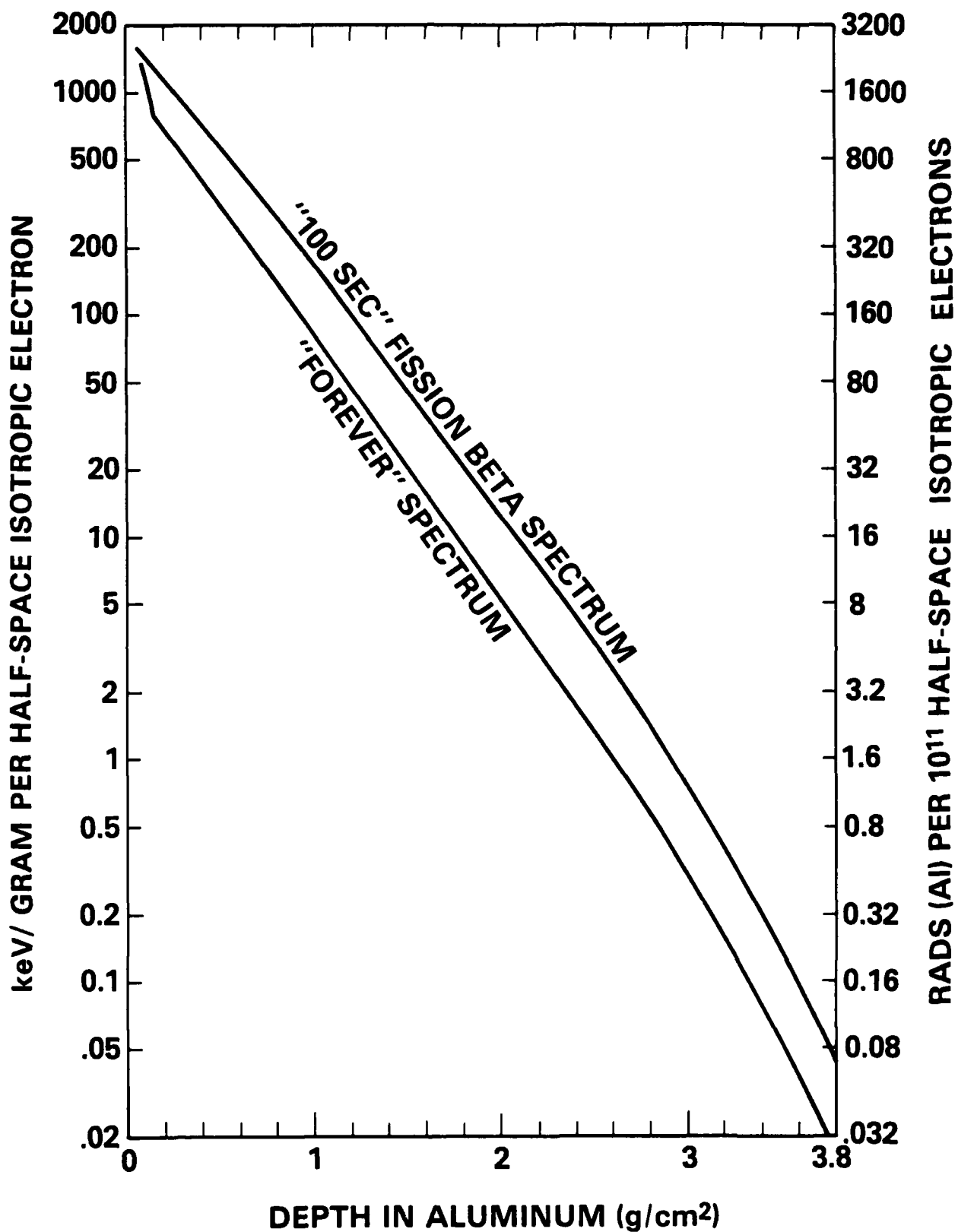
12

Fig. 2 Energy deposition in a slab of aluminum by isotropic
fission beta particles.

13

Appendix A

SPECTRAL SHAPE

The data of Table 2 were matched with the form

$$1000\ Y = (M - T)^h\ e^p, \qquad\qquad (A1)$$

where $p = a_0 + bT + cT^2$. $\qquad\qquad (4)$

More precisely, data were to be fitted with a different value of p for each of many regions. The exact form of the maximum-energy term is of no great consequence as the induced changes in the parameters of the exponent p largely compensate for them.

The final forms use the cutoff term $(9 - T)$ and six sets of parameters. First, the three central energy integrals, E, were utilized to determine the parameters for the region from 1.8 to 3.0 MeV. Thereafter, one boundary value of Y and two E values can be used to calculate each additional set of parameters. While five trios will fill this prescription, rather sharp changes in slope occurred at some boundaries, so an additional set of parameters was employed on the high energy side. As can be seen in Fig. 1, a distinct change in slope occurs at 0.9 MeV with the long-time case. The accuracy of the rather arbitrary fitting procedure is suggested by comparing the values in Table 2 with those of a preliminary fit. The 100-second average data, with $(8.5 - T)$ as the cutoff term and a different fitting procedure, produced 2.52 and 2.60 keV/fission for the 0.0-0.1 and 7.5-8.5 MeV regions, respectively.

The input energy integrals, E, were not rounded as in Table 2. Rather, the "100-second" cases were rounded to 3 decimal digits; the "forever" cases, to 5 significant figures. The 22 output values all agree with the corresponding inputs within one in the last digit, and all but one agree within 5 parts in 10^6. The differences in y at the 10 boundaries between equation ranges are all less than 12 parts in 10^6. All of this is far more accurate than necessary in view of the underlying data and/or various assumptions.

Appendix B

DISCRETE SPECTRA

The method employed to obtain the equivalent discrete spectrum is given here. The basic idea is quite simple; it is essentially the inverse of integration by Simpson's rule. The procedure is more complex when one attempts (a) to present rounded numbers in the output with a minimum loss of accuracy and (b) to avoid the high-low alternation of values characteristic of the inverse Simpson's rule solution.

The discrete spectrum is required to have the same <u>sums</u> of particles, energy, and (energy)^2 as the <u>integrals</u> of Eq. (6). Consider a set of regions of width 2r and the region centered on $T = x$. One has

$$Z_k = \int_{x-r}^{x+r} 1000y\ T^k\ dT \tag{6a}$$

for $k = 0$, 1, and 2. Set these equal to values obtained for discrete components L, M, and U at the lower limit, midpoint, and upper limit, respectively. The equations are

$$Z_0 = L + M + U, \tag{B1}$$

$$Z_1 = L(x-r) + Mx + U(x+r), \tag{B2}$$

$$\text{and}\quad Z_2 = L(x-r)^2 + Mx^2 + U(x+r)^2. \tag{B3}$$

Solve first for U, obtaining

$$2Ur^2 = (Z_1 - Z_0 x)r + Z_2 - 2Z_1 x + Z_0 x^2. \tag{B4}$$

One may then use this value of U in (B1) and (B2) to obtain M:

$$Mr = (Z_1 - U(x+r)) - (x-r)(Z_0 - U). \tag{B5}$$

Finally, one may solve (B1) for L.

In rounding off U to whatever number of digits is desired in the output value (e.g., Table 4), one alters the value of M and L. In rounding off M, the value of L is again changed. The rounded values of the three components do not quite equal the Z's; the residuals should be combined with the values for the next region in order to produce compensating roundings. (In practice, it is convenient to subtract off only the M and U contributions to the Z's, letting L be part of U for the next region.) Start with the highest energy region and proceed down in energy.

15

The above procedure leads to M components about twice as large as the others. (This is analogous to the 1,4,2,4,2... weighting for integration by Simpson's rule.) This may be avoided by use of a duplicate set of solutions using regions bounded by the midpoints of the first set. The average of the two solutions will not have the alternate high-low characteristic. One of these sets will extend beyond the desired lower limit. For the case here, one final region will be from 0.5 to -0.5 MeV. The component at -0.5 MeV must be shifted to 0.0, 0.5, and 1.0 so as to fit the three conditions.

If the table is to consist of integers, each set of solutions must be rounded to even integers. Suppose that the calculations produce U = 4.62 in one set and M = 10.84 as its mate in the second set. By rounding to U = 4 and M = 10, one obtains an average A = 7. A better answer is obtained by solving the two sets of solutions in synchronism. In the example, first calculate the average A = 7.73, then round it off to the integer A = 8. As the increase is 0.27, the individual values are increased to U = 4.89 and M =11.11.

A Hewlett-Packard 97 calculator was programmed to calculate the discrete spectra, as outlined above. The input integrals are for 0.5-MeV bins, which are then paired differently for the two synchronous solutions.

Appendix C

ENERGY DEPOSITION BY ISOTROPIC MONOENERGETIC ELECTRONS

The energy deposited by electrons in aluminum, both directly and via bremsstrahlung, is treated by Watts and Burrell.[4] In particular, we utilize their Monte Carlo results on direct energy deposition by isotropic monoenergetic electrons. Slab geometry is used, with sufficient back shielding to stop all electrons. The parameters are initial kinetic energy, T, and the depth as a fraction, F, of the average pathlength, P.

Watts and Burrell perform a series of Monte Carlo calculations, tracing a large number of electrons at each of six angles of incidence, to produce the depth-dose relationship for each of eight electron energies. It is emphasized that the results are given per half-space isotropic electron; that is, for $(\cos\theta)_{av} = 0.5$ electron incident upon the surface. Although an integration of the energy deposition shows only about 90 percent of the energy, the addition of reflection and bremsstrahlung produce the proper result.

Reference 4 calculates dose, W, from the integral over depth bins of 0.02 pathlengths. In this report, the Ref. 4 values are smoothed in order to reduce the statistical fluctuations inherent in Monte Carlo calculations. In the conversion equation, the integration over bin size is also undone and Table 5 lists the value at the point F. The equation utilized is

$$24\ Q(F) = 14\ W(F) + 7\ W(F+.02) + 7\ W(F-.02)$$

$$- 2\ W(F+.04) - 2\ W(F-.04). \tag{C1}$$

As expected, the data given by Watts and Burrell show great fluctuations near full depth. In the present report, the dose at such depths is an analytic function fitted to the last part (11 to 15 values) of the Monte Carlo results. The form adopted and given in Table 6 is

$$Q(F) = k\ (D-F)^{3.5}, \tag{C2}$$

where k is in units of keV/gram. Note that some high-energy electrons penetrate to depths beyond the average pathlength. These are electrons which have not experienced a significant bremsstrahlung event. At lower energies, this effect is less important than repeated angular scattering, and all depths reached are less than the average pathlength.

17